Enhancing low cost stainless steel implants: bioactive silica-based sol-gel coatings with wollastonite particles

Josefina Ballarre*

INTEMA – Universidad Nacional de Mar del Plata,
Juan B Justo 4302, B7608FDQ Mar del Plata,
Buenos Aires, Argentina
Fax: 54-223-4810046
E-mail: jballarre@fi.mdp.edu.ar
and
Max Planck Institute of Colloids and Interfaces,
Department of Biomaterials,
14476 Potsdam, Germany
*Corresponding author

Yifei Liu

Max Planck Institute of Colloids and Interfaces,
Department of Biomaterials,
14476 Potsdam, Germany
and
Department of Medical Physics in Radiology,
German Cancer Research Center,
Im Neuenheimer Feld 280,
69120 Heidelberg, Germany
E-mail: Yifei.Liu@dkfz-heidelberg.de

Emigdio Mendoza

Universidad Nacional de Colombia,
Calle 59A # 63-20, Medellín, Colombia
E-mail: emigdio.mendoza@upb.edu.co

Hanna Schell

Julius Wolf Institute and Center for Musculoskeletal Surgery,
Charité – University Medicine Berlin,
Augustenburger Platz 1, 13353 Berlin, Germany
E-mail: Hanna.Schell@charite.de

Facundo Díaz and Juan Carlos Orellano

Traumatología y Ortopedia,
Hospital Interzonal General de Agudos 'Oscar Alende',
Juan B. Justo y 167, 7600 Mar del Plata, Argentina
E-mail: facurdiaz@hotmail.com
E-mail: servicio.oyt.higa.mdp@gmail.com

Peter Fratzl

Max Planck Institute of Colloids and Interfaces,
Department of Biomaterials,
14476 Potsdam, Germany
E-mail: Peter.Fratzl@mpikg.mpg.de

Claudia García

Universidad Nacional de Colombia,
Calle 59A # 63-20, Medellín, Colombia
E-mail: cpgarcia@unal.edu.co

Silvia M. Ceré

INTEMA – Universidad Nacional de Mar del Plata,
Juan B Justo 4302, B7608FDQ Mar del Plata,
Buenos Aires, Argentina
E-mail: smcere@fi.mdp.edu.ar

Abstract: A hybrid organic-inorganic sol-gel coating with the addition of wollastonite particles is used as a potential solution to improve performance of low cost AISI 316L stainless steel. This work is focused on characterising the coatings by studying their synthesis and deposition, electrochemical, and *in vitro* and *in vivo* response. The coated implants presented *in vitro* Ca/P-rich apatitic precursors phases on their surface and acceptable electrochemical behaviour. The *in vivo* response regarding bone formation seems to be excellent either with the implant in contact with bone marrow, in contact with the endostium or in contact with the trabecular bone. The bioactive and regenerative responses of bone tissue to the TEOS-MTES-wollastonite system over-compensate the coating deterioration reaction, making these coatings as a good way to improve osseo-integration of stainless steel for long term use implants.

Keywords: stainless steel; bioactive coatings; bone formation; corrosion; osteo-integration; SAXS.

Reference to this paper should be made as follows: Ballarre, J., Liu, Y., Mendoza, E., Schell, H., Díaz, F., Orellano, J.C., Fratzl, P., García, C. and Ceré, S.M. (2012) 'Enhancing low cost stainless steel implants: bioactive silica-based sol-gel coatings with wollastonite particles', *Int. J. Nano and Biomaterials*, Vol. 4, No. 1, pp.33–53.

Biographical notes: Josefina Ballarre is a Material Engineer and Material Science Doctor. She is currently an Assistant Researcher from the National Council of Scientific and Technical Investigations (CONICET, Argentina) and Teacher in the materials field at the National University of Mar del Plata. Her interests include sol-gel coatings, corrosion, bioactivity, nanoindentation, bone regeneration and inorganic characterisation of bone tissue.

Yifei Liu received her PhD in Biophysics in 2010 from Humboldt University of Berlin, Berlin, Germany, her MS in Medical Physics in 2006 from the University of Heidelberg, Heidelberg, Germany, and her BS in Biomedical Engineering in 2005 from Shanghai Jiaotong University, Shanghai, China. She is currently working in the German Cancer Research Center, Heidelberg, Germany, and is involved in a research project on materials for tissue regeneration within systemically altered bone.

Emigdio Mendoza obtained his Master in Science at the Universidad Nacional de Colombia in 2009. His thesis was based on the synthesis and characterisation of bioactive coatings on metallic substrates. Actually, he is a doctoral student at the Universidad Pontificia Bolivariana in Medellín Colombia. His research interest is in metals used as biomaterials.

Hanna Schell is a Veterinarian (DVM). She received her doctoral grade from Charité, Universitätsmedizin – Berlin. She is currently holding a postdoctoral research position at the Julius Wolff Institute, Charité, Universitätsmedizin – Berlin with research interests including bone and defect healing, as well as cartilage healing. Her main focuses are establishing suitable animal models and radiological, histological and biomechanical analysis methods.

Facundo Díaz is a Medical Doctor with the specialisation in Orthopedic and Trauma. His is currently in the permanent staff of the Department of Orthopedics and Traumatology of the HIGA Hospital in Mar del Plata, Argentina. His research interest covers surgical procedures for total hip replacements, optimisation and implementation of implants and new materials.

Juan Carlos Orellano is a Medical Doctor. He is an Orthopeadic specialist and the Chief of the Orthopedics and Traumatology Department of HIGA Hospital since 1992. His fields of interest are new materials as bone and joint replacements, oseointegration and tissue regeneration. Also, he studies the different ways to improve the injury treatment and the ways to preserve the integrity of the patient.

Peter Fratzl is a Professor Dr. Dr. Honoris Causa and Engineer. He is the Director of the Department of Biomaterials of the Max Planck Institute of Colloids and Interfaces, Potdam, Germany. He has won many awards and distinctions including, in 2008, the max Planck Prize together with Prof. Robert Lange, MIT, for pioneering work in the field of 'biological and biommimetic materials'. He has published more than 300 scientific works in the fields of biommimetic materials, bone and mineral research for biomedical applications and, mechanical properties and modelling of composites materials.

Claudia García is a Materials Scientist and Engineer. She received her PhD from the Universidad Autónoma de Madrid, Spain. She is a Professor of the Universidad Nacional de Colombia. Her research interests are base on synthesis and structural and biological characterisation of ceramics and glass biomaterials and coatings.

Silvia M. Ceré is a Chemical Engineer and PhD in Material Sciences by the National University of Mar del Plata, Argentina. She is an Adjunct Professor, full-time, at the National University at Mar del Plata and staff member of the National Research Council, (CONICET, Argentina). Her research activities involve the surface modification of metals used as implant materials and environmentally friendly coatings applied on industry used alloys.

1 Introduction

The skeleton of the human body is subjected to strong mechanical solicitations and for load-bearing applications metals are the most frequently used materials for orthopaedic permanent implants. They have the best weight/dimension/mechanical properties relationships for this use (Jacobs et al., 1998; Bowditch and Villar, 2001). Metals such as stainless steels (AISI 316L, 317L), Cr-Co alloys (ASTM F-75, F-799) and Ti-based alloys (Ti-6Al-4V, ASTM F-136) are employed in total replacement osseoarticular surgeries. In developing countries, and especially in Latin America, the need of reduction in public health services has conducted to the massive use of stainless steel for permanent orthopaedic implants as the cheapest option although in most developed countries this option was leaved behind (Villamil et al., 2002; Disegi and Eschbach, 2000). It has been reported that corrosion events on the surface of the implant lead over time to a reaction with the environment of the implant (Milosev, 2002; Pan et al., 2000; Shih et al., 2004), surrounding it with fibrous tissue and eventually leading to rejection of the foreign body (Katti, 2004; Mc Geachie et al., 1992; Walczak et al., 1998). Some metallic materials are protected from the physiological media by generating a protective barrier, which can block the contact to the solution, thus avoiding the release of particles and ions from the corrosion processes into the body fluids (Hashem, 2003; Messaddeq et al., 1999; Neumann et al., 1998; Chou et al., 2001). Surface modification of surgical implants is often used as a tool to generate a surface that besides being protective could also allow the integration of the metal to the human body, creating a bioactive surface (Rodríguez et al., 2008; Krupa et al., 2003; Yang et al., 2004; Im et al., 2007). It is then of great importance to develop techniques that enhance the corrosion resistance and bioactivity of these materials, and to study its bonding with the muscular and skeletal systems. With the use of porous metallic coatings on metals, the adherence problems between the implants and the adjacent tissue are trying to be solved (Simmons et al., 1999; Otsuki et al., 2006). Other possibility is the surface modification of the metallic implants with inorganic ceramic or glassy coatings as a way to improve the implant performance. One type of coatings that shows biocompatibility is the silica-based type with silane precursors (Chou et al., 2001). The attainments of films by the sol-gel process have been successfully used on stainless steel, silver and aluminium; and have improved the oxidation and corrosion resistance of those metals (de Sanctis et al., 1990, 1995). It is possible to replace some inorganic components for organic ones, giving more plasticity to the structure (Galliano et al., 1998; Amato et al., 2005; Ballarre et al., 2007) leading to a better adaptability to the substrate surface and to the possibility of adding particles to the coating, reinforcing or functionalising it as an attempt to provide the metallic substrate a bone-like formation and adhesion to the existing structure.

In particular, titanium implants coated with plasma sprayed wollastonite, $CaSiO_3$, (Xue et al., 2005; Liu et al., 2001; Liu and Ding, 2002) or filled with wollastonite in powder form (Sahai and Anseau, 2005) have been proven to have *in vitro* hydroxyapatite deposition ability, bone compatibility, osseo-conductivity and also bone inductivity in contact with bone marrow but the bone structure of the new formed tissue is still not evaluated. The quality of the newly formed bone tissue between the implants and the existing one is of great importance for the early fixation of the prosthesis, as well as a possible way to evaluate the performance of bioactive materials as bone formers for cement-less orthopaedic devices.

The aim of this work is to characterise a sol-gel TEOS-MTES coating with the addition of wollastonite particles as potentially bioactive particles on surgical grade stainless steel *in vitro* in terms of bioactiveness and corrosion response, as well as to analyse its *in vivo* osseo-integration ability and the quality of the generated bone tissue around the implants. The coatings are made with the objective of bio-activate the surface of the AISI 316L stainless steel cement-less prosthesis, giving them the ability to generate high quality bone tissue for the implant fixation, present acceptable corrosion behaviour and still remain low cost when compared with other alloys, for being competitive with the market existing prosthesis.

2 Experimental details

2.1 Materials

Stainless steel AISI 316L (Atlantic Stainless Co. Inc., Massachusetts, USA) in the form of wires (0.15 cm diameter and 2 cm length) and plates ($3 \times 2 \times 0.2$ cm^3) were used as substrates. The composition of the steel was: C 0.03% max, Mn 2% max, Si 1% max, P 0.045% max, S 0.03% max, Ni 10% to 14%, Cr 16% to 18%, Mo 2% to 3%, and balance Fe. The wires and plates were degreased, washed with distilled water and rinsed in ethanol before coating.

Hybrid organic-inorganic sols were prepared by acid catalysis using tetraethylorthosilane (TEOS, 99%, ABCR GmbH & Co, Germany) and methyltriethoxy-silane (MTES, 98%, ABCR GmbH & Co, Germany) as precursors and absolute ethanol as solvent. The molar ratio of the silanes was maintained constant (TEOS/MTES = 40/60), fixing R in 2, where $R = H_2O/(SiO_2)$. Nitric acid (0.1 $mol.L^{-1}$) and acetic acid was used as catalysers. The sol was prepared by constant stirring at 300 rpm at 40 ºC for 3 h.

To analyse the optimum particle percentage to generate the suspension, sedimentation curves were used. Different amounts of commercial wollastonite particles (NYAD 1250, Minera NYCO SA, USA) were added (from 3% to 10% wt.) to the previously prepared sol. The commercial wollastonite particles were mainly needle shape, with an average size (D50) of 3.5 μm and with an asymmetric mono-modal distribution . Also several dispersants (Silane 6011, SILIQUEST A-1100, phosphate ester and hydroxide of tetrapropyl ammonium) were tested to choose the best one. The suspensions were stirred applying high shear mixing in a rotor-stator agitator (Silverson L2R, UK) for 4 min.

Coatings were obtained by the dip-coating technique at room temperature and withdrawn at 4 cm.min^{-1}. Double-layer coatings were applied on the substrates in two steps. The first layer prepared with TEOS-MTES sol was obtained at room temperature by dip-coating at a withdrawal rate of 4 cm.min^{-1}, dried at room temperature for 0.5 h, and then heat treated for 0.5 h at 450^{o}C in an electric furnace in air. The second layer of TEOS-MTES with 10 wt% wollastonite particles was applied on top of the first layer using the same withdrawal rate and thermal treatment than for the coatings without the particles. The integrity of the coatings was evaluated by optical microscopy (Olympus BX41, USA) and the thickness was measured using digital holographic microscopy technique using a JAI CV-M4+CL (USA) camera and an acquisition card CORECO X64-CL (USA).

2.2 In vitro analysis

Coated plates were tested for apatite deposition by immersion in simulated body fluid solution (SBF), which contained the amount of inorganic ions present in the human plasma (Kokubo et al., 1990), for a total of 33 days, with a surface area/solution volume ratio equal to 0.3 cm^2/mL. The solution was refreshed every 8 days to avoid precipitation (Kokubo and Takadama, 2006). The samples were retrieved at different periods of time. After the immersion, they were rinsed with distilled water and dried in air. The surfaces were observed using a scanning electronic microscope (SEM, Jeol JSM-5910V, Japan).

XRD tests were made on the samples using Mg Kα (1253.6 eV) radiation, a current of 50 mA, voltage of 40 kV, scan step size of 0.02 and a time per step of 0.5 seconds (XRD, Philips X'Pert MPD).

2.3 Electrochemical assays

Electrochemical assays were conducted in a PCI4 750/potentiostat/galvanostat/ZRA^{TM} (Gamry Instruments, USA). A conventional three electrode cell was used with a saturated calomel electrode (SCE; radiometer, France) as reference electrode and a platinum wire as counter electrode. All electrochemical assays were held with SBF as electrolyte and after stabilisation of the corrosion potential (Ecorr) for at least 24 h. Potentiodynamic polarisation curves were conducted from Ecorr to 1.4 V and backwards, or up to a maximum current density of 1μA cm^{-2}, at a sweep rate of 0.002 V s^{-1}. Electrochemical impedance spectroscopy (EIS) test were registered at the Ecorr with an amplitude of 0.01 V rms sweeping frequencies from 20000 to 0.01 Hz. Impedance data fitting was performed using Zplot for Windows (1998) software. Electrochemical test were conducted after 1, 7 and 40 days of immersion in SBF.

2.4 In vivo experiments

2.4.1 Surgical implantation

In vivo experiments were conducted in total on 4 Hokkaido adult rats (weighted 350 ± 50 g), according to the codes and rules of the Ethics Committee of the National University of Mar del Plata (Interdisciplinary Committee, April 2005), taking care of surgical procedures, pain control, standards of living and appropriated death. The protocol and

implantation procedure was explained elsewhere (Ballarre et al., 2011). Briefly, the coated and uncoated stainless steel implants were sterilised in an autoclave for 20 minutes at 121°C, rats were anaesthetised with fentanyl citrate and droperidol (Janssen-Cilag Lab, Johnson and Johnson, Madrid, Spain) according to their weight. The coated and bare implants were placed by press fit into the femur, extending them into the medullar canal. The animals were sacrificed with an overdose of intraperitoneal fentanyl citrate and droperidol, after 60 days when the bones with implants were a bladed. Conventional X-ray radiographs were taken before retrieving the samples for control purposes.

2.4.2 Samples sectioning

The retrieved samples (femurs) were cleaned from surrounding soft tissues and fixed in neutral 10 wt% formaldehyde for 24 h. Then they were dehydrated in a series of acetone-water mixture followed by a methacrylate solution and finally embedded in methyl methacrylate (PMMA) solution and polymerised. The PMMA embedded blocks were cut with a low speed diamond blade saw (Buehler GmbH) cooled with water. Various sections were made according to different analysis: 300 to 450 μm thick sections for small angle X-ray scattering (SAXS) measurements and 200 μm thick sections for histological staining. Care was taken to keep the samples surface as free from scratches as possible. The femurs were cut at four different levels to compare the bone ingrowth (Figure 1). The BC cut shows the trabecular bone present in the epiphysis and the CD, DE and EF cuts show the cortex compact bone.

Figure 1 Scheme of the femur sections analysed for the *in vivo* essays

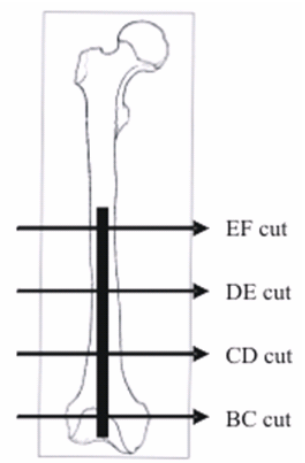

2.4.3 Histological analysis

To observe the hard tissue and the bone lining cells, the histological sections were stained with 20% Giemsa stain solution (Bradbeer et al., 1994). The stained sample sections were observed using optical light microscope (Leica DM RXA2, Germany).

2.4.4 SAXS analysis

SAXS samples were mounted on a sample holder perpendicularly to the X-ray beam path. A computer-controlled stage enables movement of the sample in two directions (x and y) within the sample plane. Before scattering measurements, a radiograph was generated by measuring the transmitted X-ray intensity with a pin-diode placed behind the sample while scanning the whole sample area with a step size of 0.1 mm and an accumulation time of 1 s at each step. The SAXS measurement points were chosen from the radiograph to be mostly in the newly formed bone region at the periphery of the implant and few in the old cortex for comparison. X-ray beam was generated by a rotating Cu-anode generator (M06XCE-SRA, Mac Science, Japan) operating at 40 kW, 100 mA (Cu Kα radiation, wavelength 1.5418 Å), collimated by an evacuated double pinhole system, and collected by a position-sensitive area detector (HI-STAR, Bruker AXS, Karlsruhe, Germany). Acquisition time of scattering data was 3,600 s for each measured position. The size of the X-ray beam was 200 μm at the sample plane and the sample-to-detector distance was about 60 cm. All the spectra were corrected for background scattering and detector noise. The calibration of the beam centre position on the detector was done by measuring scattering signal from silver behanate (AgBh) calibrant. The reduction of data from two-dimensional SAXS pattern to one-dimensional intensity curve was done by Fit2D programme (2-dimensional data analyser, ESRF, France). Further analysis for obtaining information on mineral particle thickness and orientation was done using a self-developed-based programme.

The integration of the 2D SAXS data can be done either radially or azimuthally to eventually obtain the mineral thickness (T-parameter) (Fratzl et al., 1991) and the degree of alignment of the mineral particles (ρ-parameter) (Rinnerthaler et al., 1999). The predominant orientation can be calculated from the anisotropy of the SAXS pattern.

3 Results and discussion

3.1 Sol, suspension and coatings characterisation

A transparent and colourless TEOS-MTES sol was obtain, with a pH of 2 and a viscosity of 3.6 cP that did not present variations over a 15 days test period. There was neither change in the physical properties and nor evidence of gelation or precipitation, indicating a good stability of the sol with time (García et al., 2005).

To analyse particles suspension, different quantities of the particles (3% to 10% wt.) were added to the sol and analysed with sedimentation curves, without the addition of any dispersant agent (Figure 2). With a 3% and 5% of solids the sedimentation percentage reaches asymptotic values, but when the load is raised to 10%wt of wollastonite particles without any dispersant, the sedimentation process occurs at high rate and after a few minutes a gelification event can be noticed, with an abrupt rise of viscosity (figure not shown) and the formation of a solid mass of gel plus wollastonite particles.

Figure 2 Sedimentation curves for the TEOS-MTES sol with the addition of 3 (■), 5 (•) and 10 (▲) %wt. of wollastonite particles

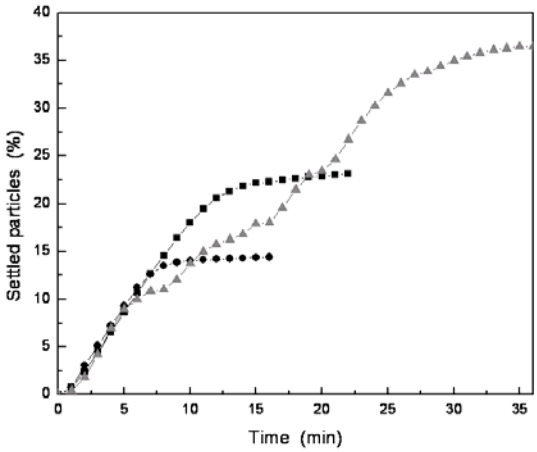

Figure 3 shows the sedimentation curves for the dispersants studied when the suspension contains 3%wt of wollastonite. It can be observed that the SILIQUEST A-1100 dispersant shows the highest sedimentation rate (higher than without dispersant), which indicates that the particles are suffering coalescence or agglomeration, increasing the solution instability.

Figure 3 Effect of the different type and quantity of dispersant agents during the sedimentation of suspensions prepared with 3%wt. wollastonite particles in TEOS-MTES sol

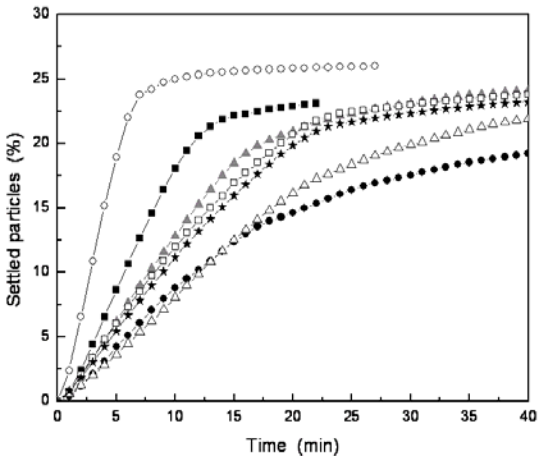

Notes: Dispersants: silane 6011 (□), SILIQUEST A-1100 (○), phosphate ester 3% (•) and 6% (Δ), hydroxide of tetrapropyl ammonium 4.3% (▲) and 8.6% (ι), and without dispersant agent (■).

The use of dispersant agents such as Silane 6011, phosphate ester or hydroxide of tetrapropyl ammonium, decreases the sedimentation rate of the wollastonite particles in the TEOS-MTES sol. The most notorious effect was reached with the 3%wt. of phosphate ester in relation with the percentage of solids (Figure 4). This agent acts over the particles generating electrostatic repulsion effects and a steric impediment, what can be translated in a decrease in the suspension sedimentation rate. By the addition of the phosphate ester as a dispersant agent, a 15%wt. of solids can be suspended in the sol without showing gelification due to the diminish of the viscosity generated by the reagent (Maiti and Rajender, 2002; Becker and Cannon, 1990). After the analysis of the different suspensions and dispersants, the choose one to make the coatings was made with 10%wt. of wollastonite particles and 3%wt. of particles of phosphate ester as dispersant agent, in the TEOS-MTES sol.

Figure 4 Sedimentation curves of the TEOS-MTES sol with the addition of different percentage of wollastonite particles [3% (■), 8% (•). 10% (▲) and 15% (▼)], with 3%wt. of phosphate ester as dispersant agent

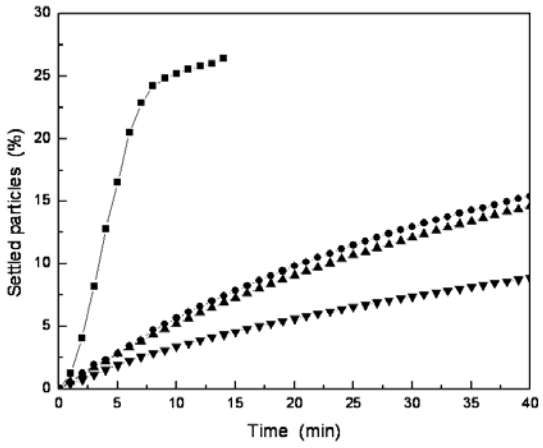

The integrity and general aspect of the coatings deposited without and with wollastonite particles using phosphate ester as dispersant can be seen in Figure 5. Figure 5(a) corresponds to a single layer TEOS/MTES coating and the Figure 5(b) to a double-layer system containing wollastonite particles. As it can be observed in the image, the particles are not forming agglomerates, showing the effect of the phosphate ester as dispersant.

The average thickness for the double-layer with the dispersion of wollastonite particles was 1.1 ± 0.05 μm.

The TEOS-MTES with wollastonite particle coatings appear homogeneous without flaws or cracks on the surface or around the wollastonite particles when observed under an optical microscope.

In previous work (Ballarre et al., 2008), the nanomechanical properties of TEOS-MTES coatings without the addition of any particles had been studied using instrumented nanoindentation, showing values of reduced modulus of 6.5 ± 0.3 GPa and 212 GPa for the stainless steel. The mean values of elastic modulus for trabecular and cortical bone in dry conditions (Hengsberger et al., 2002) are 24.0 ± 2.3 GPa and 20.5 ± 2.3 GPa, respectively, indicating the importance in having a coating with elastic reduced modulus similar to the existing bone to avoid elastic mismatch. No study was

made of the TEOS-MTES with bioactive particles; since the system is in the *micro-scale* while the measurement in the *nano*. Also, the study of coating adherence and frictional behaviour is of great importance for an orthopaedic permanent implant and it has been analysed in previous works (Ballarre et al., 2009a, 2009b) showing the excellent adhesion and good elasto-plastic recovery of the hybrid TEOS-MTES coatings under scratch tests at ambient conditions.

Figure 5 Morphologic aspect of double layer coating without, (a) and with 10% of dispersed wollastonite particles (b) without immersion in SBF

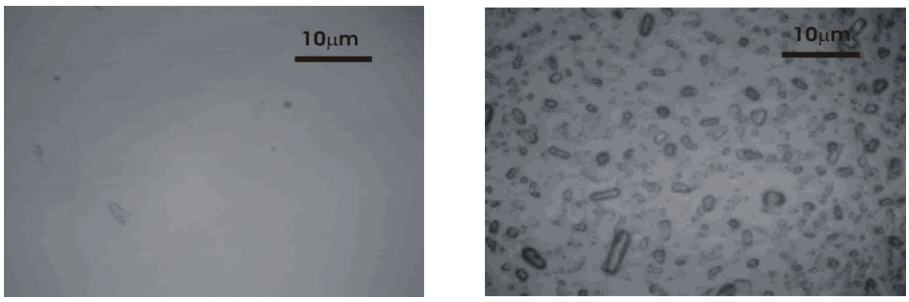

(a) (b)

3.2 In vitro analysis

In the *in vitro* tests, an apatite-like layer was formed on the surface of the TEOS-MTES-wollastonite coatings after immersion in SBF. After five days of immersion, the deposition starts with cracking and dissolution around the wollastonite particles within the TEOS-MTES coating (Figure 6). This is due to the reaction between the calcium and the hydrated silica ions that provides favourable sites for apatite nucleation and an increase in the ion activity product of the apatite in the surrounding body fluid (Garcia et al., 2004; Kokubo et al., 1992; Hench and Wilson, 1993). After 33 days of immersion, the deposited phase presented a more homogeneous island shaped appearance [Figure 7(a)]. Dissolution of the wollastonite particles provides Ca and P enrichment of the deposited phase, hence enhancing solidification (Hastings, 1980; Zhang et al., 2003). The energy-dispersive X-ray spectroscopy [EDS, Figure 7(b)] measurements confirm that this new phase is mainly composed of Ca and P, as well as the XRD diffractogram [Figure 7(c)].

Figure 6 Morphologic aspect of the double layer coating with 10% of dispersed particles of wollastonite after five days of immersion in SBF

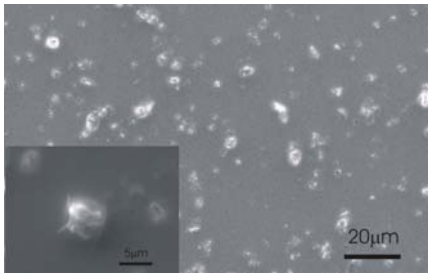

Figure 7 SEM image, (a) EDS spectra (b) XRD diffractogram of the precipitate formed on the double layer coating with 10% of dispersed particles of wollastonite after 33 days of immersion in SBF

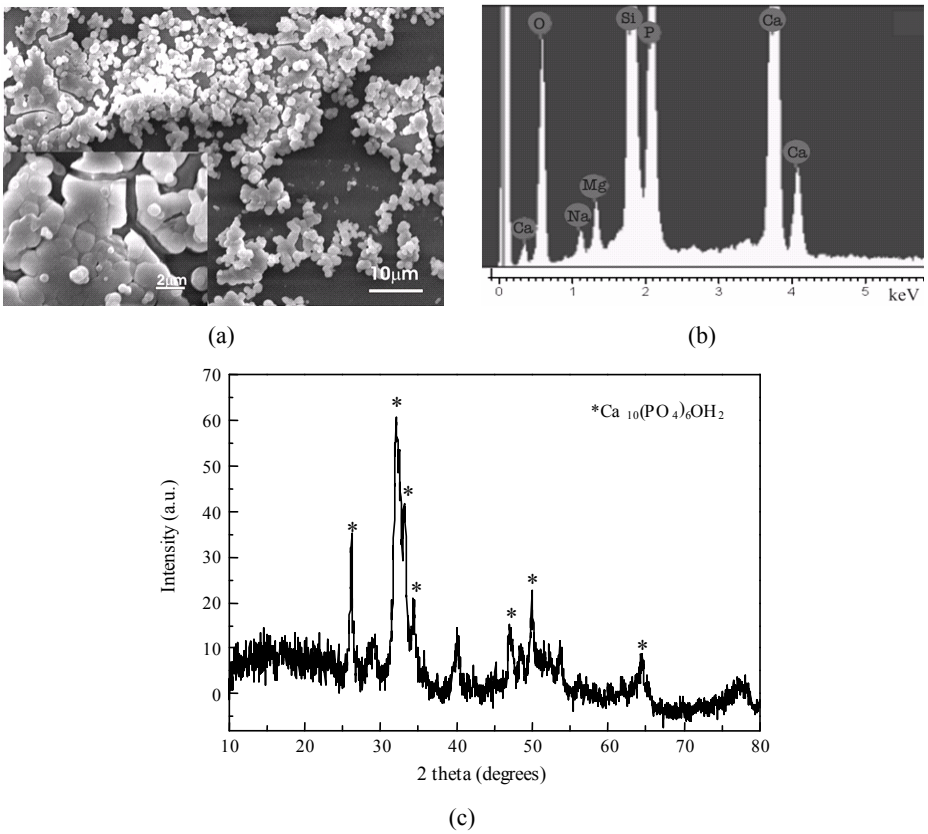

Even the apatite formation in SBF is a well known in vitro practise and a needed experiment to prove bioactivity according to the ISO 23317:2007(E) (2007) "Implants for surgery — In vitro evaluation for apatite-forming ability of implant materials", the immersion test is controversial. Several authors agreed that the solution and the way of the materials are tested, are not correct and it is not necessary the only way to prove the material's bioactivity (Bohner and Lemaitre, 2009). The surface state of the tested materials should be well characterised, and identical in both in vivo and in vitro tests.

3.3 Electrochemical assays

The corrosion behaviour of the coated materials was studied in comparison to the bare material by potentiodynamic assays and EIS.

Figure 8 shows the potentiodynamic polarisation curve for the TEOS-MTES coating with wollastonite particles after 1, 7 and 40 days of immersion in SBF and its comparison with the bare material. After 1 day of immersion, the coated material presented a low current density (i_{pass}) showing a blocking and protective behaviour of the TEOS-MTES

coating with wollastonite particles. After 7 and 40 days of immersion, the measured current density does not show noticeable differences when comparing the coated with the bare material. However, an enhancement in the breakdown potential (E_b) is observed for the coated samples, not showing localised corrosion in the range of potentials under study. Table 1 shows the most important electrochemical parameters to compare the performance of the coatings in time.

Figure 8 Potentiodynamic curves for the bare material (•), and the TEOS-MTES coating with wollastonite particles after 1 (○), 7 (□) and 40 (■) days of immersion in simulated body fluid

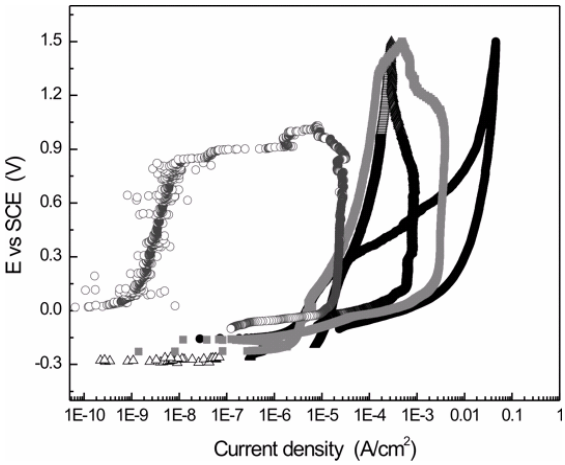

Table 1 Electrochemical parameters obtained from the potentiodynamic curves for the SS coated samples

	Naked material	*1 day immersion*	*7 days immersion*	*40 days immersion*
Eoc (V)	–0.16	0.05	–0.25	–0.17
ipass (A/cm2)	5×10^{-6}	3×10^{-9}	2×10^{-6}	2×10^{-6}
Eb (V)	0.3	1.5	1.5	0.8

Figure 9 shows the EIS plots in Bode representation of the samples coated with TEOS-MTES containing wollastonite particles and a comparison with the bare stainless steel. After 1 day of immersion, the coated material presents a highly capacitive behaviour showing high total resistance impedance that could be related with the coating integrity. With the increase in the immersion time (7 days), the coatings present a notorious general deterioration due to the breaking and dissolution of the particles in the coating. After 40 days of immersion in SBF, the system showed a similar behaviour than after 7 days due to continuous cracking of the coating and the porous Ca/P compounds deposition on the created defects (Keding et al., 2002).

When comparing coated with uncoated samples, the barrier effect provided by the sol el coating showed to improve the resistance to localised corrosion although the current density after prolonged immersion remains constant.

Figure 9 Bode representation for the EIS studies for the SS316L substrate (•), TEOS-MTES coated materials with wollastonite particles after 1 (○), 7 (□) and 40 (■) days of immersion in simulated body fluid

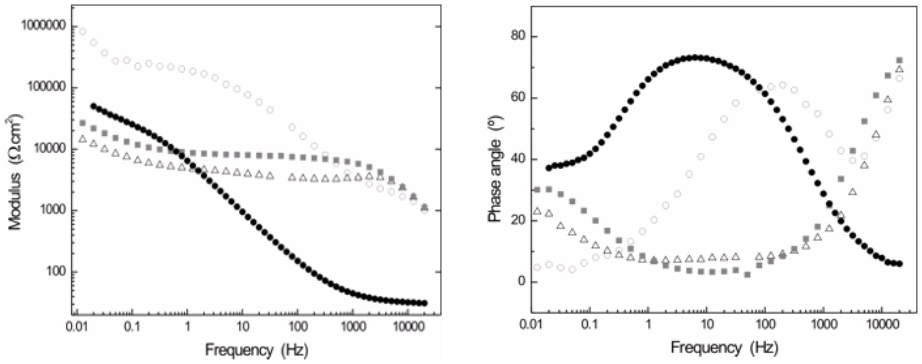

3.4 Histological analysis

Figure 10 shows the optical microscopic images of Giemsa stained sections of the implanted TEOS-MTES coatings with wollastonite particles samples after 60 days of implantation in rat femurs. Figure 10(a) illustrates the BC section, where the trabecular bone of the epiphysis is the predominant tissue. Some bone tissue formation can be denoted on the periphery of the implant in isolated islands [Figure 10(b)]. About 60% of the newly formed bone is in contact with the metallic implant, as calculated based on image analysis techniques (Image J software).

In Figure 10(c), a newly formed bridge-like bone tissue can be seen between the implant and the existing cortical bone endostium: this is known as the re-modelling zone between the implant and the old cortex bone. The cortex can be distinguishing from the newly formed bone by its structure and by its laminar morphology. Newly grown bone tissue can be identified around the implant growing in contact with the bone marrow. The growth direction of lamellar bone tissue seems to be perpendicular to the longer axis of the nail-like implant, and perpendicular to the existing cortical bone.

After 60 days of implantation, the newly-formed tissue around the implant is completely mature, presenting osteoid and osteocyte lacunae, pointed out with white arrows in Figure 10(d). However, it also possesses a laminar structure with an osteoblast-rich (osteoid layer) surface near the implant, marked also in Figure 10(d). That shows a continuous bone growth by concentric bone apposition by intramembranous-type ossification.

Bone formation in the periphery of the coated implants demonstrates that the TEOS-MTES coatings with wollastonite particles show osseo-induction in contact with the existing bone as well as with the marrow. It can be seen that there is bone growth in the narrowest gaps between the old cortex and the implant as well as bone regeneration around the implant. This shows that the coating is fixed to the existing tissue and that it generates newly formed bone in its periphery. However, it can be seen that bone tissue is only partially attached to the implant, as is expected at the early stages of bone regeneration.

Figure 10 Optical microscopic images of giemsa stained histology sections showing the coated implant and the newly formed bone for: the BC cut with, (a) 5x and (b)10x, the CD cut level (c)10x and (d)40x magnification, after 60 days of implantation in rat femur (see online version for colours)

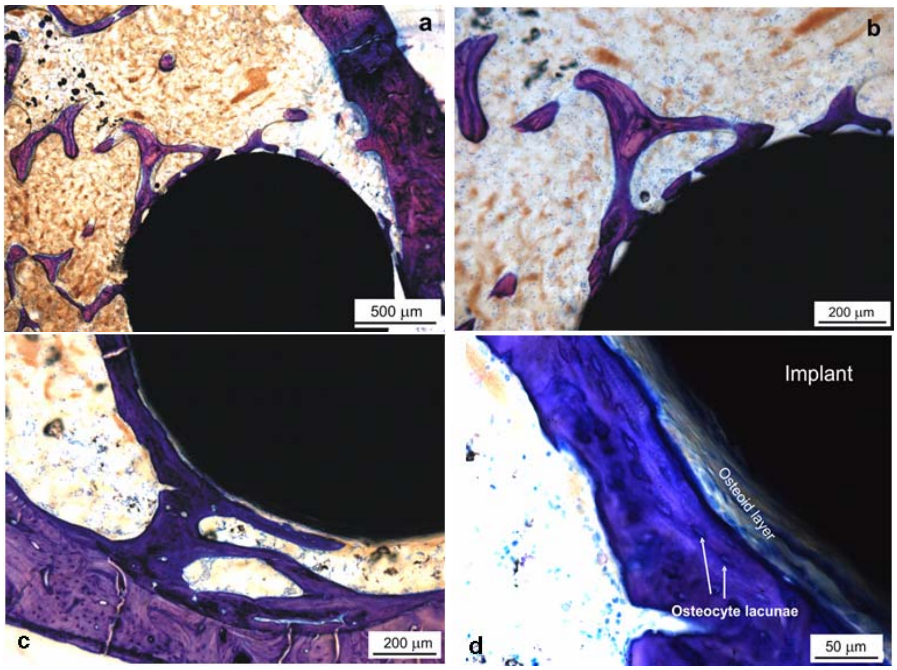

Figure 11 Optical microscopic image of giemsa stained histology section showing the naked stainless steel implant after 60 days of implantation (10x) (see online version for colours)

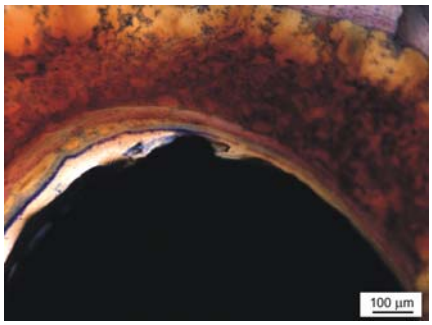

The histology images showed in Figure 10 indicate new bone tissue growth around the implant at different cut levels, as it was indicated in Figure 1. This tissue seems to have not differences in terms of generation and formation between the growth sites in contact with the endostium (remodelation zone) or in contact with the bone marrow. A lamellar growth of collagen tissue with osteoblastic presence can be seen at the periphery of the zone implant-tissue. This structure cannot be observed with the metallic implant without coating (Figure 11), where an apparently fibrous tissue that encapsulates the implant with a single osteoblastic cell layer can be observed. This case means an unacceptable weak

bone fixation of the implant, as revealed by the loose space between fibrous tissue and metal. Theses results confirm that the surgical grade stainless steel by itself is not able of inducing bone growth *in vivo* on its surface, even after 60 days of implantation.

3.5 SAXS measurements

Figure 12 shows two typical SAXS graphs presenting the X-ray scattering intensity diffraction of the sections of the implanted TEOS-MTES coatings with wollastonite particles samples after 60 days of implantation in rat femurs. In each cut level analysed, several points of the samples were picked for T and ρ parameter analysis. The points were chosen from the old cortex tissue, from the remodelation zone between the implant and the cortical bone, and from the implant in contact with the marrow. T parameter mean values and its deviation for each zone are shown in Table 2. ρ parameter is expressed as white bars in the X ray intensity plots.

Table 2 *T* parameter values for the bone tissue formed around the implant and of the existing cortical bone of the different cut levels studied

Region	*T parameter Cortex (mean ± SD)*	*T parameter near implant (mean ± SD)*
Femur BC	2.14 ± 0.15 nm	2.03 ± 0.07 nm
Femur CD	2.46 ± 0.15 nm	2.13 ± 0.10 nm
Femur DE	2.30 ± 0.11 nm	2.06 ± 0.20 nm
Femur EF	2.36 ± 0.10 nm	2.04 ± 0.14 nm

The mean thickness of the Ca/P rich crystals (T) was evaluated at the different femur cut levels studied (as described in Figure 1). Differences were found in the bone zones in contact with the bone marrow and in contact with the cortex compact bone. The *T* parameter showed higher values for the cortical bone zone, which presents a high degree of mineralisation, and lower values for the newly-formed bone. All the samples at different cutting levels presented the same mean thickness of the crystals in the new bone tissue, which indicates that the osseo-inductive effect of the implant does not depend on the level of the bone where the implant is placed. The difference falls in the amount of new bone generated around the implant (Figure 8).

The ρ parameter, can be seen in Figure 12(a) and Figure 12(b) for BC and CD femur cut levels respectively. The length of the bar denotes the degree of alignment of the particles (ρ-parameter) and direction of the bar gives the overall preferred orientation of the mineral particles. Since the mineral particles (HAp) in the bone structure are aligned with the longitudinal axis of the collagen fibrils, ρ gives also information about the orientation of this organic matrix (Fratzl et al., 1996). It can be seen that the newly formed bone around the coated implant at the different levels BC and CD have the mineral crystals preferentially orientated parallel to the direction of the existing bone and following the circumference of the implant. The BC cut shows the implant in contact with a trabecular bone environment, presents highly orientated apatite-like crystals. It is worth noting that at both cut levels, the mineral particles in the old cortex follow the architecture of the bone and are aligned with the direction of bone growth. These results are in agreement the histology analysis showing mature newly formed bone plenty of

osteoid lacunae near the TEOS-MTES with wollastonite particles implant at both trabecular and cortical bone levels.

Figure 12 Radiograph of the cuts, (a) BC (b) CD of the femur with the coated implant after 60 days of implantation measured with SAXS showing the intensity of the transmitted X-ray through the sample section

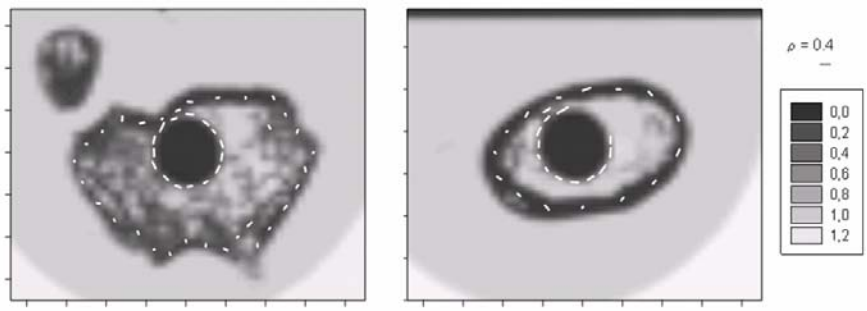

(a) (b)

Notes: The small white bars denotes the degree of orientation of the mineral particles in the measured spots around the implant, the size of bar denotes the degree of alignment and the direction of the bars denotes the orientation of the mineral particles.

In previous work, the effect of glass ceramic particles of the system P_2O_5-CaO-SiO_2 in a TEOS-MTES coating with different content of silica nanoparticles, was analysed *in vivo* (Ballarre et al., 2010) showing also highly orientated apatite crystals around the implant at the diaphysis level with a low amount of SiO_2 nanoparticles in the coating. The bone induction and growth near silica-based sol-gel with wollastonite particles coating indicate that the presence of calcium silicate particles plays a key role in increasing the bioactivity of the coating of metallic implants. Regarding apatite formation in the presence of silica, some related results were presented by Li et al. (1992) showing the catalytic effect of Si-OH groups for the apatite nucleation that promote the formation of apatite in silica gels immersed in SBF. The *in vivo* effect of calcium silicate coatings in the oseo-integration was already found with a silica-rich interlayer between the old and the newly formed bone (Xue et al., 2005). The use of wollastonite particles as a disperse phase in sol-gel protective coatings is presented as a way to improve stainless steel bioactivity at low cost and with an enhancement of implant fixation at different levels.

The use of this kind of coatings applied on cement-less orthopaedic prosthesis have good clinical perspectives since they are able to promote implant fixation creating a continuous formed new bone while the corrosion resistance of the substrate remains stable.

4 Conclusions

The use of wollastonite particles as a disperse phase in sol-gel protective coatings, improve stainless steel bioactivity at low cost. The presence of calcium silicates particles plays a key role in bone induction and formation. It enhances bone growth around the implant at different levels and does not deteriorate corrosion resistance of the implant

after immersion in SBF. Furthermore, the bioactive and regenerative responses of bone tissue to the TEOS-MTES-wollastonite system over-compensate the coating deterioration reaction in time, making these coating as a good way to improve osseo-integration of stainless steel for long term use implants.

References

Amato, L.E., López, D.A., Galliano, P.G. and Ceré, S.M. (2005) 'Electrochemical characterization of sol-gel hybrid coatings in cobalt-based alloys for orthopaedic implants', *Materials Letters*, Vol. 59, No. 16, pp.2026–2031.

Ballarre, J., Jimenez-Pique, E., Anglada, M., Pellice, S. and Cavalieri, A.L. (2009a) 'Mechanical characterization of nano-reinforced silica based sol-gel hybrid coatings on AISI 316L stainless steel using nanoindentation techniques', *Surface and Coatings Technology*, Vol. 203, No. 20, pp.3325–3331.

Ballarre, J., López, D.A. and Cavalieri, A.L. (2009b) 'Frictional and adhesive behavior of organic-inorganic hybrid coatings on surgical grade stainless steel using nano-scratching technique', *Wear*, Vol. 266, Nos. 11–12, pp.1165–1170.

Ballarre, J., López, D.A. and Cavalieri, A.L. (2008) 'Nano-indentation of hybrid silica coatings on surgical grade stainless steel', *Thin Solid Films*, Vol. 516, pp.1082–1087.

Ballarre, J., López, D.A., Schreiner, W.H., Durán, A. and Ceré, S.M. (2007) 'Protective hybrid sol-gel coatings containing bioactive particles on surgical grade stainless steel: surface characterization', *Applied Surface Science*, Vol. 253, No. 17, pp.7260–7264.

Ballarre, J., Manjubala, I., Schreiner, W.H., Orellano, J.C., Fratzl, P. and Ceré, S. (2010) 'Improving the osteointegration and bone-implant interface by incorporation of bioactive particles in sol-gel coatings of stainless steel implants', *Acta Biomaterialia*, Vol. 6, No. 4, pp.1601–1609.

Ballarre, J., Seltzer, R., Mendoza, E., Orellano, J.C., Mai, Y.W., García, C. and Ceré, S.M. (2011) 'Morphologic and nanomechanical characterization of bone tissue growth around bioactive sol-gel coatings containing wollastonite particles applied on stainless steel implants', *Materials Science and Engineering C*, Vol. 31, No. 3, pp.545–552.

Becker, R.E. and Cannon, W.R. (1990) 'Source of water and its effect on tape casting barium titanate', *Journal of the American Ceramic Society*, Vol. 73, No. 5, pp.1312–1317.

Bohner, M. and Lemaitre, J. (2009) 'Can bioactivity be tested in vitro with SBF solution?', *Biomaterials*, Vol. 30, No. 12, pp.2175–2179.

Bowditch, M. and Villar, R. (2001) 'Is titanium so bad? Medium – term outcome of cemented titanium stems', *The Journal of Bone & Joint Surgery (Br)*, Vol. 83-B, pp.680–685.

Bradbeer, J.N., Riminucci, M. and Bianco, P. (1994) 'Giemsa as a fluorescent stain for mineralized bone', *Journal of Histochemistry and Cytochemistry*, Vol. 42, No. 5, pp.677–680.

Chou, T.P., Chandrasekaran, C., Limmer, S.J., Seraji, S., Wu, Y., Forbess, M.J., Nguyen, C. and Cao, G.Z. (2001) 'Organic-inorganic hybrid coatings for corrosion protection', *Journal of Non-Crystalline Solids*, Vol. 290, Nos. 2–3, pp.153–162.

de Sanctis, O., Gómez, L., Pellegri, N. and Durán, A. (1995) 'Behaviour in hot ammonia atmosphere of SiO2-coated stainless steels produced by a sol-gel procedure', *Surface and Coatings Technology*, Vol. 70, Nos. 2–3, pp.251–255.

de Sanctis, O., Gomez, L., Pellegri, N., Parodi, C., Marajofsky, A. and Duran, A. (1990) 'Protective glass coatings on metallic substrates', *Journal of Non-Crystalline Solids*, Vol. 121, pp.338–343.

Disegi, J.A. and Eschbach, L. (2000) 'Stainless steel in bone surgery', *Injury, Int. J. Care Injured*, Vol. 31, pp.2–6.

Fratzl, P., Fratzl-Zelman, N., Klaushofer, K., Vogl, G. and Koller, K. (1991) 'Nucleation and growth of mineral crystals in bone studied by small-angle X-ray scattering', *Calcified Tissue International*, Vol. 48, No. 6, pp.407–413.

Fratzl, P., Schreiber, S. and Boyde, A. (1996) 'Characterization of bone mineral crystals in horse radius by small-angle X-ray scattering', *Calcified Tissue International*, Vol. 58, No. 5, pp.341–346.

Galliano, P., De Damborenea, J.J., Pascual, M.J. and Duran, A. (1998) 'Sol-gel coatings on 316L stainless steel for clinical applications', *Journal of Sol-Gel Science and Technology*, Vol. 13, pp.723–727.

Garcia, C., Ceré, S.M. and Durán, A. (2004) 'Bioactive coatings prepared by sol-gel on stainless steel 316L', *Journal of Non-Cristalline Solids*, Vol. 348, pp.218–224.

García, C., Durán, A. and Moreno, R. (2005) 'Stability of suspensions of bioactive particles using hybrid organic-inorganic solutions as dispersing media', *Journal of Sol-Gel Science and Technology*, Vol. 34, pp.1–7.

Hashem, K.M.E. (2003) 'Study of TEOS and TPOS anticorrosion coatings developed at different ranges of pyrolisis temperatures', *Applied Surface Science*, Vol. 217, pp.302–313.

Hastings, G.W. (1980) 'Biomedical engineering and materials for orthopaedic implants', *Journal of Physics E: Scientific Instruments*, Vol. 13, No. 6, pp.599–607.

Hench, L.L. and Wilson, J. (1993) *An Introduction to Bioceramics: Advanced Series in Ceramics – World Scientific*, edited by Hench, L.L. and Wilson, J., Vol. 1.

Hengsberger, S., Kulik, A. and Zysset, P. (2002) 'Nanoindentation discriminates the elastic properties of individual human bone lamellae under dry and physiological conditions', *Bone*, Vol. 30, No. 1, pp.178–184.

Im, K-H., Lee, S-B., Kim, K-M. and Lee, Y-K. (2007) 'Improvement of bonding strength to titanium surface by sol-gel derived hybrid coating of hydroxyapatite and titania by sol-gel process', *Surface and Coatings Technology*, Vol. 202, Nos. 4–7, pp.1135–1138.

International Standard ISO 23317:2007(E) (2007) Implants for surgery – in vitro evaluation for apatite-forming ability of implant materials, Switzerland.

Jacobs, J.J., Jeremy, M.D., Gilbert, J.L. and Urban, R.M. (1998) 'Current concept review – corrosion of metal orthopaedic implants', *The Journal of Bone & Joint Surgery, Incorporated*, Vol. 80, No. 2, pp.268–282.

Katti, K.S. (2004) 'Biomaterials in total joint replacement', *Colloids and Surfaces B*, Vol. 39, pp.133–142.

Keding, R., Rüssel, C., Pascual, M.J., Pascual, L. and Durán, A. (2002) 'Corrosion mechanism of borosilicate sealing glasses in molten carbonates studied by impedance spectroscopy', *Journal of Electroanalytical Chemistry*, Vol. 528, Nos. 1–2, pp.184–189.

Kokubo, T. and Takadama, H. (2006) 'How useful is SBF in predicting in vivo bone bioactivity?', *Biomaterials*, Vol. 27, pp.2907–2915.

Kokubo, T., Kushitani, H., Ohtsuki, C. and Sakka, S. (1992) 'Chemical reaction of bioactive glass and glass – ceramics with a simulated body fluid', *Journal of Materials Science: Materials in Medicine*, Vol. 3, pp.79–83.

Kokubo, T., Kushitani, H., Sakka, S., Kitsugi, T. and Yamamuro, T. (1990) 'Solutions able to produce in vivo surface – structure changes in bioactive glass – ceramic', *A. W. Journal of Biomedical Materials Research*, Vol. 24, pp.721–734.

Krupa, D., Baszkiewicz, J., Sobezak, J.W., Bilinski, A. and Barcz, A. (2003) 'Modifying the properties of titanium surface with the aim of improving its bioactivity and corrosion resistance', *Journal of Materials Processing Technology*, Vols. 143–144, pp.158–163.

Li, P., Ohtsuki, C., Kokubo, T., Nakanishi, K., Soga, N., Nakamura, T. and Yamamuro, T. (1992) 'Apatite formation induced by silica gel in simulated body fluid', *Journal of the American Ceramics Society*, Vol. 75, No. 8, pp.2094–2097.

Liu, X. and Ding, C. (2002) 'Morphology of apatite formed on surface of wollastonite coating soaked in simulate body fluid', *Materials Letters*, Vol. 57, No. 3, pp.652–655.

Liu, X., Ding, C. and Wang, Z. (2001) 'Apatite formed on the surface of plasma-sprayed wollastonite coating immersed in simulated body fluid', *Biomaterials*, Vol. 22, No. 14, pp.2007–2012.

Maiti, A.K. and Rajender, B. (2002) 'Terpineol as a dispersant for tape casting yttria stabilized zirconia powder', *Materials Science and Engineering A*, Vol. 333, Nos. 1–2, pp.35–40.

Mc Geachie, J., Smith, E., Roberts, P. and Grounds, M. (1992) 'Reaction of skeletal muscle to small implants of titanium or stainless steel: a quantitative histological and autoradiographic study', *Journal of Biomedical Materials Research*, Vol. 13, No. 8, pp.562–568.

Messaddeq, S.H., Pulcinelli, S.H., Santilli, C.B., Guastaldi, A.C. and Messaddeq, Y. (1999) 'Microstructure and corrosion resistance of inorganic-organic (ZrO2-PMMA) hybrid coating on stainless steel', *Journal of Non-Crystalline Solids*, Vol. 247, pp.164–170.

Milosev, I. (2002) 'Effect of complexing agents on the electrochemical behavior of orthopaedic stainless steel in physiological solution', *Journal of Applied Electrochemistry*, Vol. 32, pp.311–320.

Neumann, H.G., Beck, U., Drawe, M. and Steinbach, J. (1998) 'Multilayer systems for corrosion protection of stainless steel implants', *Surface and Coatings Technology*, Vol. 98, pp.1157–1161.

Otsuki, B., Takemoto, M., Fujibayashi, S., Neo, M., Kokubo, T. and Nakamura, T. (2006) 'Pore throat size and connectivity determine bone and tissue in growth into porous implants: three-dimensional micro-CT based structural analyses of porous bioactive titanium implants', *Biomaterials*, Vol. 27, No. 35, pp.5892–5900.

Pan, J., Karlen, K. and Ulfvin, C. (2000) 'Electrochemical study of resistance to localized corrosion of stainless steel for biomaterial applications', *Journal of the Electrochemical Society*, Vol. 147, No. 3, pp.1021–1025.

Rinnerthaler, S., Roschger, P., Jakob, H.F., Nader, A., Klaushofer, K. and Fratzl, P. (1999) 'Scanning small angle X-ray scattering analysis of human bone sections', *Calcified Tissue International*, Vol. 64, No. 5, pp.422–429.

Rodríguez, H.H., Vargas, G. and Cortés, D.A. (2008) 'Electrophoretic deposition of bioactive wollastonite and porcelain-wollastonite coatings on 316L stainless steel', *Ceramics International*, Vol. 34, No. 5, pp.1303–1307.

Sahai, N. and Anseau, M. (2005) 'Cyclic silicate active site and stereochemical match for apatite nucleation on pseudowollastonite bioceramic-bone interfaces', *Biomaterials*, Vol. 26, No. 29, pp.5763–5770.

Shih, C-C., Shih, C-M., Su, Y-Y., Su, L.H.J., Chang, M-S. and Lin, S-J. (2004) 'Effect of surface oxide properties on corrosion resistance of 316L stainless steel for biomedical applications', *Corrosion Science*, Vol. 46, pp.427–441.

Simmons, C.A., Valiquette, N. and Pilliar, R. (1999) 'Osseointegration of sintered porous-surfaced and plasma spray-coated implants: an animal model study of early postimplanation healing response and mechanical stability', *Journal of Biomedical Materials Research*, Vol. 47, pp.127–138.

Villamil, R.F.V., Aranha, H., Chaves De Andrade Alfonso, M.L., Tomanik Mercadante, M. and Leite Agostinho, S.M. (2002) 'Stainless steels in orthopaedic implants: fundaments and corrosion resistance', *Rev. Bras. Ortop.*, Vol. 37, Nos. 11–12, pp.471–476.

Walczak, J., Shahgaldi, F. and Heatley, F. (1998) 'In vivo corrosion of 316L stainless steel hip implants: morphology and elemental composition of corrosion products', *Biomaterials*, Vol. 19, pp.229–237.

Xue, W., Liu, X., Zheng, X. and Ding, C. (2005) 'In vivo evaluation of plasma-sprayed wollastonite coating', *Biomaterials*, Vol. 26, No. 17, pp.3455–3460.

Yang, B., Uchida, M., Kim, H-M., Zhang, X. and Kokubo, T. (2004) 'Preparation of bioactive titanium metal via anodic oxidation treatment', *Biomaterials*, Vol. 25, No. 6, pp.1003–1010.

Zhang, Y., Mizuno, M., Yanagisawa, M. and Takadama, H. (2003) 'Bioactive behaviours of porous apatite- and wollastonite-containing glass-ceramic in two kinds of simulated body fluid', *Mater. Res. Soc.*, Vol. 18, pp.433–441.

Zplot for Windows (1998) *Electrochem Impedance Software Operating Manual: Part 1*, Scribner Ass. Inc., Southern Pines, NC.